EUROMECH - 2nd European Nonlinear Oscillation Conference
Prague, September 9-13, 1996

CHAOTIC BEHAVIOR IN A GENERALIZED CLOSED LOOP THIRD ORDER DRIVEN SYSTEM WITH NONLINEAR GAIN

Leo J. **Stocco** and A.C. **Soudack**
Department of Electrical Engineering, The University of British Columbia
Vancouver, British Columbia, Canada V6T 1Z4
(Fax: (604) 822-5949; E-mail: leos@ee.ubc.ca)

Abstract

A model of a generalized third order negative feedback system with three finite poles, all zeros at infinity and a nonlinear gain function is driven with a sinusoidal input. The response of the system is studied for different initial open loop pole placement locations and gain coefficients. Under a wide range of parameter values, the system is observed to exhibit periodic, multi-periodic and chaotic behavior with unique fractal patterns embedded in some of the bifurcation diagrams. The Poincaré sections of the chaotic regions are also atypical since they trace finite curves rather than fill enclosed regions.

Introduction

It is proposed that unpredictable behavior will occur in a closed loop, negative feedback, third order system which is amplified by a nonlinear gain function. Since unpredictable behavior is most likely if a system is lightly damped and near instability, the excitation, gain and system parameters must be chosen suitably to induce the behavior.

System Definition

Third order systems have either three real poles or one real pole and two complex conjugates. The root locus interprets both to be special cases of the same system with different gains. A generalized system can therefore be defined as in Figure 1. Note that the system is simplified by placing all zeros at infinity.

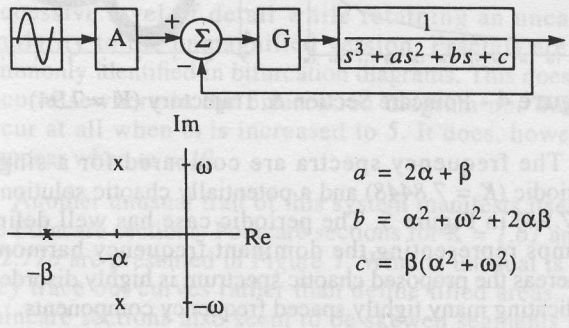

Figure 1 - Generalized Third Order System

Nonlinear Gain Function

A saturating gain function is applied to the system. Saturation is a property that exists in many real life components such as transistors and transformers so its effect on an otherwise well behaved system is of interest. Since saturation can not be represented analytically, it is approximated using the natural log function. The function is shown in Figure 2.

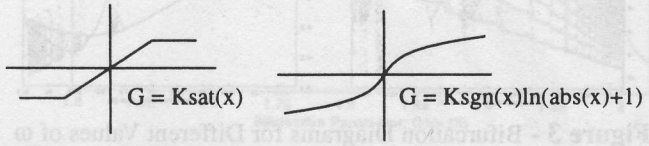

Figure 2 - Nonlinear Gain Function

The approximation always has non-zero gain for finite inputs and has no discontinuities. It is not only analytic, but is also more representative of real device behavior than the perfect saturation function and, therefore, serves as a valid model.

Parameter Selection

The system has five variables: α, β, ω, signal amplitude (A) and gain (K). K is kept independent since it can be used to place the open-loop complex poles with respect to the $j\omega$ axis which directly affects system stability. The remaining four parameters are chosen such that the system becomes unstable as slowly as possible to maximize the range of K where the system is lightly damped but stable.

This is done by maximizing the angle of the complex pole paths in the root locus so that the angle of approach between the complex poles and $j\omega$ axis is minimized. Since the asymptote angle is fixed by the number of poles, only the departure angle can be tuned by the design parameters:

$$\text{departure angle} = \text{atan}((\beta - \alpha)/\omega)$$

The departure angle increases when either β is increased or when α or ω are decreased. Since only the relationship between the parameters is important, α is normalized to *1*. Compromises are necessary for β and ω since a very large β places the real pole close to a zero and approximates a second order system and a very small ω approximates a DC input. A value of $\beta = 2$ is chosen (keeping $\beta > \alpha$ simplifies the path of the root locus) while a value for ω is sought experimentally.

Signal amplitude (A) does not affect the root locus but it must be large enough such that the system is sufficiently disturbed. A value of $A = 30$ is chosen.

Effect of Varying Input Frequency

Bifurcation diagrams for $\alpha = 1$, $\beta = 2$, $A = 30$ and $\omega = 1, 2, 5$ and 10 are presented in Figure 3. When $\omega = 1$ the solution is always periodic except when $0.95 < K < 0.99$ where the solution period doubles and when $0.99 < K < 1.03$ where the solution appears chaotic. In the apparently chaotic

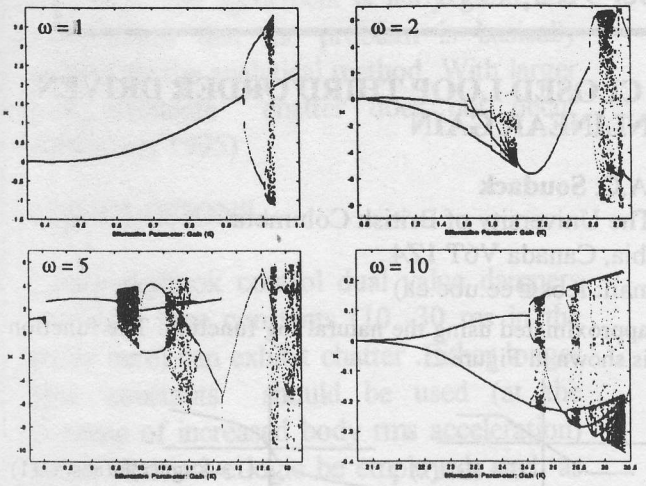

Figure 3 - Bifurcation Diagrams for Different Values of ω

regions, this disordered behavior is extremely sensitive to initial conditions. For example, at $K = 1.02$ the basin of attraction to the multi-periodic solution set extends barely beyond the solution set itself. Any significant deviation results in a solution that is periodic (period three) and centred about $\dot{x} \approx 3.2$.

When $\omega = 2$ or $\omega = 5$ there are two qualitative differences with respect to when $\omega = 1$. First, the system bifurcates from single-periodic to chaotic and back to single-periodic more than once. Second, the basins of attraction are almost infinitely large since the post-transient solutions remain unchanged for all initial conditions that maintain stability.

When $\omega = 10$ the system behavior once again becomes similar to when $\omega = 1$. Although the basin of attraction remains large, there is once again only one region of multi-periodic solutions that is delimited on either side by a single-periodic solution. The system appears to fade in and out of chaos when either K or ω are varied.

There appears to be a direct relationship between ω and the value of K required before the first bifurcation occurs. Employing the Routh-Hurwitz criterion (Phillips and Harbor 1991) on the transfer function shows that the system becomes unstable when:

$$K > 2\alpha\{\alpha(\alpha + 2\beta) + \omega^2 + \beta^2\}$$

As ω increases, a larger gain is required to make the system unstable. Since chaotic behavior is only expected in systems which are near instability, the gain required to invoke chaos should experience a similar dependence on ω. This is consistent with the observations in Figure 3. Table 1 shows approximate values of K where the first period doubling occurs, the range where chaotic behavior is observed, and the boundary value where the system becomes unstable.

Verifying Chaotic Behavior

It is important to verify that the behavior that is assumed to be chaotic is in fact so. One way is to verify that bifurcations occur abruptly and simultaneously. A second test is to see if the Poincaré sections and trajectories continue to reappear in their entirety if they are periodically

Table 1: Gain Boundary Values

ω	Gain K		
	First Bif.	Chaotic Reg.	Instability
1	0.95	0.99 - 1.03	2.64
2	0.82	1.61 - 2.83	2.97
5	7.86	7.93 - 13.37	13.37
10	21.0	24.6 - 26.4	51.5

erased. If not then it is likely that only transients are being observed. The frequency spectrum can also be analyzed since chaotic behavior incorporates many tightly spaced frequency components. Finally the Lyapunov exponents and dimension can be checked since a positive Lyapunov exponent or a non-integer Lyapunov dimension is indicative of chaotic behavior.

For the purpose of verification, ω is fixed at 5. Close inspection of the first set of bifurcations show that the system has a single-periodic solution at $K = 7.8448$ and a double-periodic solution at $K = 7.8449$. The double-periodic solution continues up to $K = 7.9064$ where a quadruple- periodic solution is observed at $K = 7.9065$. Period doubling occurs within $\Delta K = 10^{-4}$ for both of these transitions.

A Poincaré section and trajectory for $K = 7.94$ is presented in Figure 4. Since the Poincaré section forms a line which completely fills in no matter how many times it is erased, it is proposed to contain an infinite number of frequencies. It should also be pointed out that the trajectory does not fill in from the outside in or from the inside out. Individual solution cycles that are neighbors in proximity are not neighbors in time so this trajectory can also be erased continually and similar ones reappear.

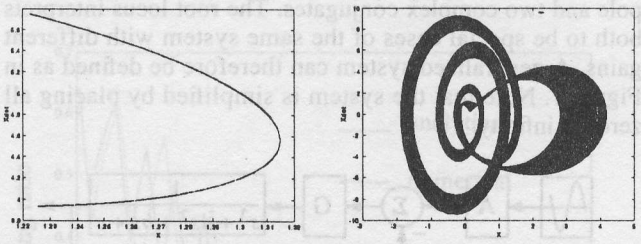

Figure 4 - Poincaré Section & Trajectory (K = 7.94)

The frequency spectra are compared for a single-periodic ($K = 7.8448$) and a potentially chaotic solution ($K = 7.94$) in Figure 5. The periodic case has well defined humps representing the dominant frequency harmonics whereas the proposed chaotic spectrum is highly disordered indicating many tightly spaced frequency components.

Finally, the Lyapunov exponents for $K = 7.94$ are $\lambda_1 = 0.0755418$, $\lambda_2 = -0.949809$ and $\lambda_3 = -2.07953$ and the Lyapunov dimension is 2.07953. The first Lyapunov exponent (λ_1) is greater than zero by about 0.08 and the Lyapunov dimension is non-integer by about 0.08. This margin is much larger than what can be reasonably expected from calculation error.

As a final precaution the entire analysis is repeated using a different integration method (Araujo *et al.* 1993).

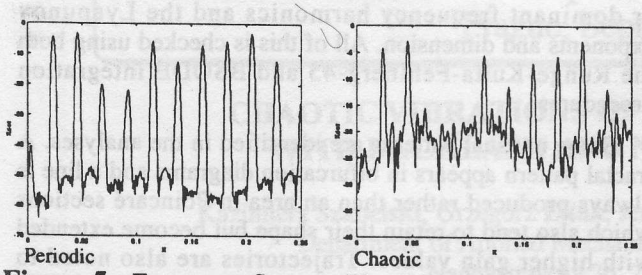

Figure 5 - Frequency Spectra (K = 7.8448, 7.94)

All of the previous simulations employed the Runge-Kutta-Fehlberg-45 integration method. They are repeated using BSODE, a stiffly stable integration procedure which is based on Gear's algorithm (Parker and Chua 1989). The resulting bifurcation diagram, Poincaré section, trajectory and frequency spectra are all similar in form to those presented in Figure 3 through Figure 5 but are somewhat noisier. The first Lyapunov exponent is also positive by about *0.05* and the Lyapunov dimension is non-integer by about *0.05*. It is therefore concluded that the solutions that were proposed to be periodic, multi-periodic and chaotic are in fact so. The Runge-Kutta-Fehlberg-45 integration procedure can therefore be used with confidence for further study. Because of its unique characteristics, ω is fixed at 2 for this purpose.

Chaotic Behavior when ω = 2

One of the most unique traits of the system emerges at values of *K* which first make the system chaotic. A magnified view of this region is presented in Figure 6. The system starts out periodic of period-2 and goes chaotic for a short time. It then returns to being periodic, but of period-3 and then goes chaotic again. It then returns to being periodic, but of period-4 and then goes chaotic again. Each time the system ceases to be chaotic, it becomes periodic of an order one higher than that before it was chaotic. The chaotic regions become thinner and more densely spaced as gain increases and the pattern repeats ad infinitum (which can be supported by further magnifications). The pattern has fractal qualities since it repeats infinitely within a bounded area and must be magnified to observe each successive level of detail while retaining an uncanny similarity to the unmagnified version. Fractals are not commonly identified in bifurcation diagrams. This does not occur elsewhere in the bifurcation diagram nor does it occur at all when ω is increased to *5*. It does, however, reappear when ω = *10*.

Another unusual trait of this system manifests itself in the Poincaré sections. Poincaré sections for *K = 1.61* and *K = 2.776* are presented in Figure 7. What is unusual is that they trace out curves rather than define filled areas. The Poincaré sections also seem to be skewed segments of a common curve which tends to get longer as *K* increases. The fact that the Poincaré sections are curves rather than areas, although uncommon, is not unique. It has been previously shown in the Henon man (Moon 1987).

Some Poincaré sections (i.e. *K = 2.776*, Figure 7) appear to almost close on themselves which would lead one to suspect periodicity. It should, however, be pointed out that since the system is third order, the Poincaré sections are actually three dimensional and have been projected onto

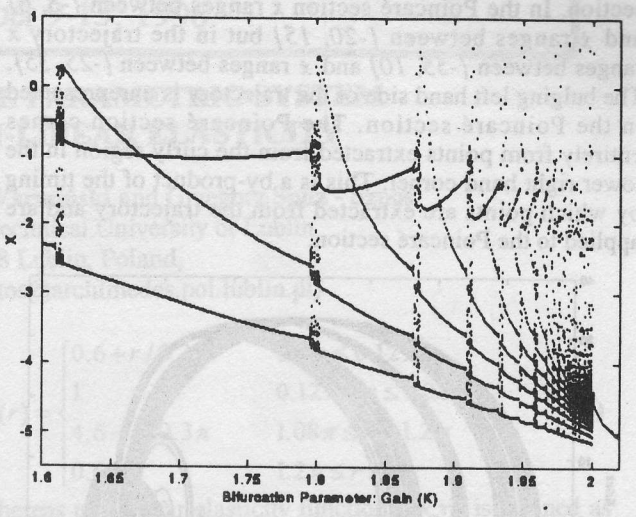

Figure 6 - Magnified Bifurcation Diagram

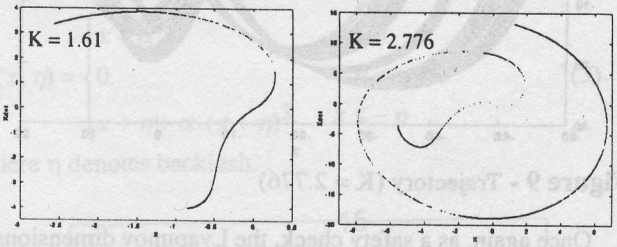

Figure 7 - Poincaré Sections

the $\dot{x}$ plane. When viewed in three-space it is clear that the Poincaré sections do not actually approach closure.

Something that is not obvious from looking at the Poincaré sections in their entirety is their actual complexity. Magnification of the *(-5.6, -3.6)* end point of the *K = 2.766* case shows that the curve does not simply end. It actually consists of three line segments, one which ends and two which join in a loop. Further magnifications do not produce any fractal-like recurrence of this pattern. A magnification of the end point is presented in Figure 8.

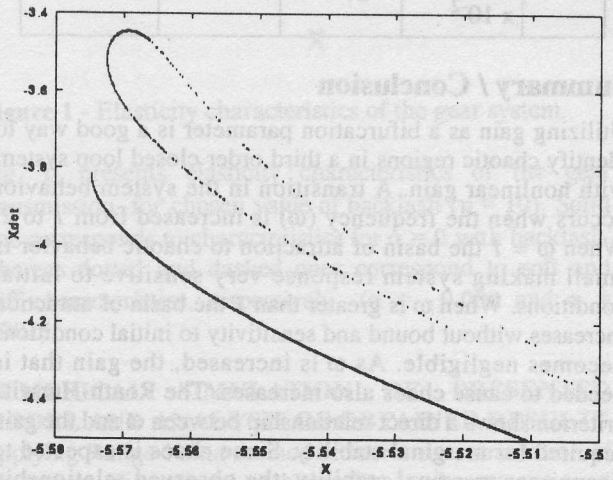

Figure 8 - End-Point Magnification of Poincaré Section

A final observation about the Poincaré sections is how they relate to their associated trajectories. A trajectory for *K = 2.766* is presented in Figure 9. What is unexpected is that the range of the trajectory far exceeds that of the Poincaré

section. In the Poincaré section x ranges between $\{-8, 6\}$ and $\dot{x}$ ranges between $\{-20, 15\}$ but in the trajectory x ranges between $\{-55, 10\}$ and $\dot{x}$ ranges between $\{-25, 35\}$. The bulging left hand side of the trajectory is unrepresented in the Poincaré section. The Poincaré section comes entirely from points extracted from the curly region in the lower right hand corner. This is a by-product of the timing by which points are extracted from the trajectory and are applied to the Poincaré section.

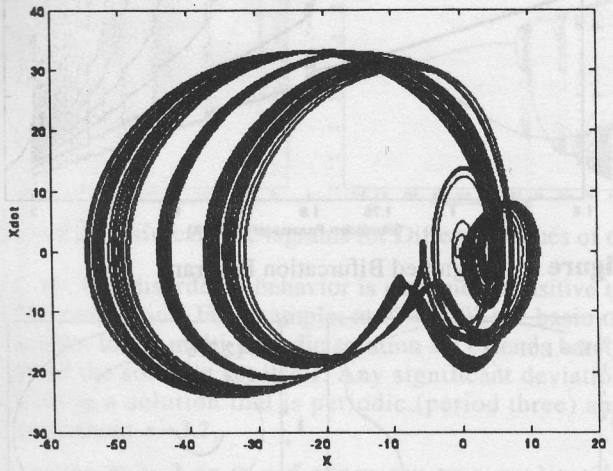

Figure 9 - Trajectory (K = 2.776)

Once again, as a safety check, the Lyapunov dimensions and exponent are calculated for the gains that were studied to ensure that there is a positive exponent and a non-integer dimension. They are presented in Table 2.

Table 2: Lyapunov Exponents and Dimensions for $\omega = 2$

Gain	Lyapunov Exponent			Lyapunov
K	λ_1	λ_2	λ_3	Dimension
1.61	3.70016 x 10^{-2}	-1.43155	-2.60546	2.02585
2.766	4.39809 x 10^{-2}	-1.654	-2.38998	2.02659

Summary / Conclusion

Utilizing gain as a bifurcation parameter is a good way to identify chaotic regions in a third order closed loop system with nonlinear gain. A transition in the system behavior occurs when the frequency (ω) is increased from *1* to *2*. When $\omega = 1$ the basin of attraction to chaotic behavior is small making system response very sensitive to initial conditions. When ω is greater than *1* the basin of attraction increases without bound and sensitivity to initial conditions becomes negligible. As ω is increased, the gain that is needed to cause chaos also increases. The Routh-Hurwitz criterion shows a direct relationship between ω and the gain required for marginal stability. Since chaos is expected to occur near marginal stability, the observed relationship between the onset of chaos, K and ω is intuitively satisfying.

After fixing the system parameters, the existence of chaos is verified by critically assessing the simultaneousness of bifurcations, the absence of transients or dominant frequency harmonics and the Lyapunov exponents and dimension. All of this is checked using both the Runge-Kutta-Fehlberg-45 and BSODE integration procedures.

Some unusual patterns are identified in the analyses. A fractal pattern appears in bifurcation diagrams and a line is always produced rather than an area in Poincaré sections which also tend to retain their shape but become extended with higher gain values. Trajectories are also noted to engulf a larger range on the phase plane than do the Poincaré sections.

Finally it is important to point out that chaotic behavior appears over a wide range of parameters (not limited to only gain and frequency as focussed on in this paper), parameter values and initial conditions. Designers of third order systems with saturating gains should therefore factor in appropriate safety factors to avoid the extensive range of problematic parameter values that have been shown to produce unpredictable and potentially chaotic results. In these systems stability and predictability are not necessarily one in the same.

References

Araujo, A.E.A.; Mozaffari, S; Soudack, A.C.; Marti, J.R. 1993, "Chaos in Power Systems: EMTP Simulations", Proc. 11th Power Systems Computation Conference, pp. 671-677.

Gleick, J. 1987, "Chaos, Making a New Science", Penguin Books.

Hilborn, R.C. 1994, "Chaos and Nonlinear Dynamics", Oxford University Press.

Moon, F.C. 1987, "Chaotic and Fractal Dynamics", John Wiley and Sons, New York, NY, 1987.

Parker, T.S.; and Chua, L.O. 1989, "Practical Numerical Algorithms for Chaotic Systems", Springer-Verlag.

Phillips, C.L. and Harbor, R.D. 1991, "Feedback Control Systems", Second Edition, Prentice Hall.

Wolf,A.; Swift, J.B.; Swinney, H.L.; Vastano, J.A. 1984, "Determining Lyapunov Exponents From a Time Series", Elsevier Science Publishers.